THE ASTROPHYSICAL JOURNAL, 305:805–813, 1986 June 15

SS 433: A 6 YEAR PHOTOMETRIC RECORD

J. C. KEMP, G. D. HENSON, D. J. KRAUS, L. C. CARROLL, AND I. S. BEARDSLEY
Department of Physics, University of Oregon
K. TAKAGISHI, J. JUGAKU, AND M. MATSUOKA
Tokyo Astronomical Observatory
AND
E. M. LEIBOWITZ, T. MAZEH, AND H. MENDELSON
Wise Observatory, Tel Aviv University
Received 1985 September 27; accepted 1985 December 5

ABSTRACT

A homogeneous record of optical photoelectric photometric measurements of this special object is presented, including over 800 observations on ~700 dates during 1979–1985, in the V band. A complete data table is furnished, which can be used for various future analyses and for correlation with other data (radio, X-ray, etc.) We present: (1) a power spectrum identifying the dominant periodicities, $13^d.081$ and $162^d.5$; (2) updated ephemerides for these periods; and (3) a mean, binned light curve on the 13 day period. Also (4), we show an interesting new synthesis of the average 162 day "precession" light curves broken down into four phase intervals on the 13 day cycle. This is a much better synthesis than was previously possible, because the well-known erratic light fluctuations in the object can now be averaged out to considerable degree. A positive "hump" at the 162^d light minimum is now clearly seen to occur around orbital phase 0.5 (secondary 13^d light minimum) but not at phase 0.0 (primary minimum). The connection with current models is discussed qualitatively.

Subject headings: stars: individual — X-rays: binaries

I. INTRODUCTION

The strange close binary system designated SS 433 = V1343 Aquilae has preoccupied observers and theorists for over six years. It is, of course, the stellar object which emits two high-speed, oppositely directed particle jets, as discovered by B. Margon and his associates (Margon 1984). Two major periodic processes are identified: (1) a supposed precession of the beams and an associated accretion disk, period of ~162 days; and (2) a 13 day orbital period. Both of these cycles were first found through spectroscopic Doppler variability, the first by Margon and co-workers, who observed large and periodic shifts of the so-called "moving" Balmer emission lines produced by the jets. The 13 day period was found by Crampton, Cowley, and Hutchings (1980), who detected small periodic shifts in the "stationary" lines which do not show the precessional motion.

Photometric variation was detected beginning in early 1979 (Gladyshev *et al.* 1979; Kemp *et al.* 1980), and light curves on both the 13 and 162 day periods have been gradually refined (Kemp *et al.* 1981; Cherepashchuk 1981; Henson *et al.* 1983; Leibowitz *et al.* 1984*b*; Gladyshev, Goranskii, and Cherepaschuk 1985). Those observations were standard photometry in broad bands, referred to comparison stars. Additionally, differential photometry in the form of line-to-continuum measurements, using the stationary Hα line, was reported by Anderson *et al.* (1983*a*). Since SS 433 is an intrinsically "noisy" object, it has taken some years to arrive at reliable, detailed mean light curves—especially in the case of the long 162^d cycle.

In this paper we record a homogeneous body of photoelectric optical photometric data, including some 800 data points on ~700 dates, spanning the period 1979 to late 1985. These data resulted from carefully coordinated programs at observatories in Oregon, Israel, and Japan. (A few special observations were also done at Mauna Kea, Hawaii.) A key contribution is our data table. This is made available to those, for example, who wish to search for correlation with other variability, e.g., radio, infrared, etc. It may be used for future analysis and modeling of the periodic processes, by others and by some of us. In the present paper, however, we will carry out only some limited synthesis of the data, and we discuss some results only qualitatively, with relationship to recent modeling by others.

II. OBSERVATIONS AND DATA

The data reported here come from a program begun at Pine Mountain Observatory (PMO), Oregon, in 1979, using the 81 cm telescope (Kemp *et al.* 1980). This effort was immediately joined by observers at Wise Observatory, Israel, using their 1 m telescope. The effort was joined in 1980 by observers at Tokyo University Observatory, Japan, using a 60 cm instrument. All of the data were taken with a common, principal comparison star which we designate star 1. A local sky chart is shown in Kemp *et al.* (1981). The chart also shows a sky-sampling position, which was adhered to throughout the program; SS 433 is a faint star ($V \approx 14$) in the Milky Way, and consistent sky sampling was crucial for accuracy. In the PMO observations, the object, sky, and comparison-star coordinates were controlled by a computer system, which made for consistency among the various observing assistants.

Standardization of star 1.—Approximate standardizations of this star were performed at PMO in 1979, 1983, and 1985, using HR (BS) stars 7303, 7288, 7266, 7219, and 7325. These are fifth to sixth magnitude stars located within a few degrees of star 1 on the sky. Using the Bright Star catalog magnitudes for these stars, we found the following V magnitudes for star 1:

JD 2,444,122.8, $V = 11.212 \pm 0.055$ (1979),
JD 2,445,563.8, $V = 11.520 \pm 0.240$ (1983),
JD 2,446,211.9, $V = 11.207 \pm 0.072$ (1985),
JD 2,446,219.9, $V = 11.291 \pm 0.033$ (1985).

A weighted mean is $V = 11.25 \pm 0.03$. The 1983 measurement was very poor and is deweighted. An independent standardization of star 1 (also other field stars near SS 433) was performed in 1981 by Leibowitz and Mendelson (1982), using Landolt standard stars. They found from four nights' data that, $V = 11.48 \pm 0.05$. Another standardization by one of us (H. M.), carried out on three nights in August 1985, gave $V = 11.44 \pm 0.02$. There appears to be an $\sim 0^m.15$ disagreement between the Oregon and Israel measures here, perhaps because of small systematic offsets between the listed magnitudes of the two groups of stars used.

On the stability of star 1: check-star measurements.—An auxiliary comparison star (check star), designated star *a*, has been observed intermittently at PMO since 1979. This star has approximate magnitude $V = 10.8$ and is located $\sim 4'$ ENE of star 1 and the "diamond" asterism (see Kemp *et al.* 1981). In the lower part of Figure 1 we show a record of 93 nights' measures of the difference $V(1) - V(a)$ over the six years. These measures were sometimes brief, and the errors were typically $0^m.04$–$0^m.10$. The possible relative variability seen in Figure 1 is quite small compared to the scale of variation in SS 433. In 1983, star 1 may appear to have been $\sim 0^m.15$ brighter, on the average, than in other years. But a rather poor standardization (see above) in 1983 suggested that star 1 may have instead been fainter, and of course it is possible that the shift in that year may have been in star *a*, not star 1. It is gratifying that we see no long-term or *secular* trend in $V(1) - V(a)$ over the six years.

a) A Six-Year Data Record of the V-Band Light Variation

A principal component of this paper is Table 1. We list here the magnitude differences V(SS 433) $- V$(star 1), with Julian dates. Observations have in fact been carried out in various filter bands (Kemp *et al* 1981; Leibowitz *et al.* 1984*b*) but on shorter time scales. Since it was found that the color dependence of the light variation is weak, it was decided that only the V observations would be continued on a long-term basis.

In Table 1, the observing stations and telescopes used are indicated as follows. Data taken at PMO (Oregon) on the 81 cm telescope carry no special notation. Letters W, K, T, or M after data points signify the following: W; Wise Observatory, Israel, 1 m telescope; K: Kagoshima Space Center, Japan, 60 cm telescope; T: Tokyo Astronomical Observatory, Okayama, Japan, 90 cm telescope; M: Mauna Kea, Hawaii, 61 cm telescope.

Note that the Okayama and Mauna Kea observations were made only in August and September 1984. A special campaign of concentrated observations was carried out at that time by the combined Oregon, Israel, and Japan teams to coincide with X-ray observations of SS 433 by the *EXOSAT* and *Tenma* satellites—and, also, to study the light variation on a nearly 24 hour basis. This campaign was organized by the Japanese group and included collaboration with the X-ray astronomy group at the University of Leicester, UK. It included special Mauna Kea observations by an extra Japanese team (Ymasaki

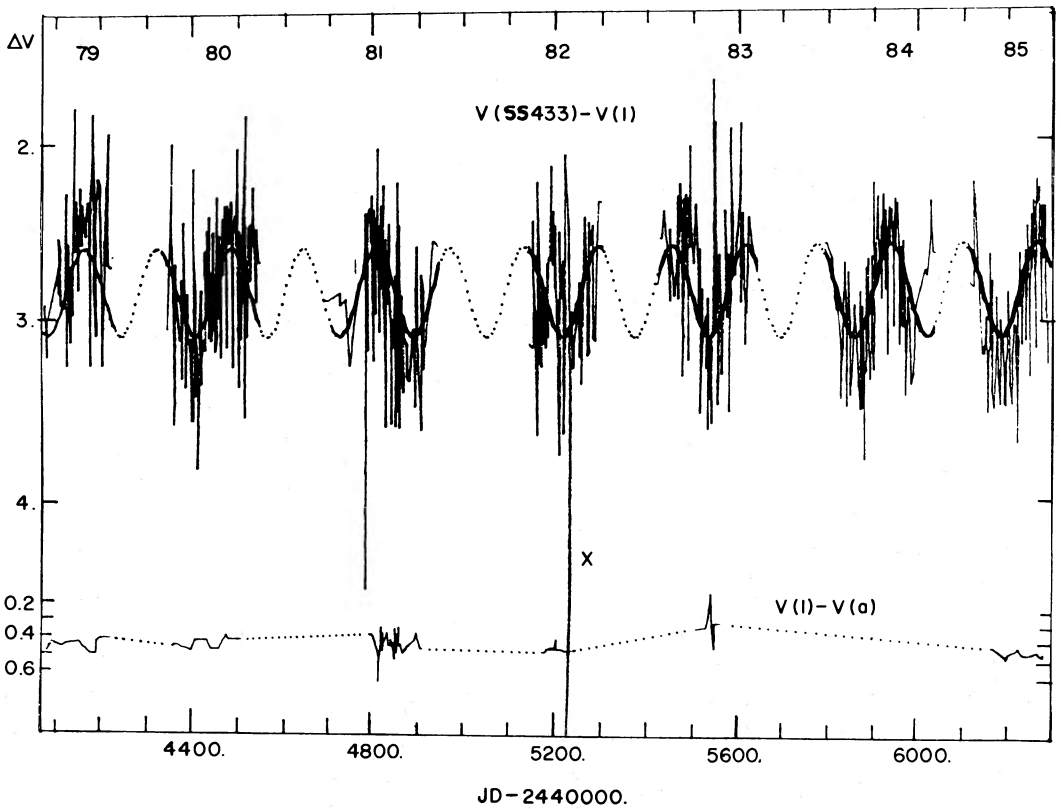

FIG. 1.—Simple, real-time plot of the V-band light variation of SS 433 during 1979–1985, in terms of the magnitude difference relative to the comparison star 1 (*see text*); an inverted scale is used, with upward meaning SS 433 is brighter. To guide the eye, we connect the data points (from Table 1) with straight-line segments. The "rapid" fluctuations are largely due to the 13 day orbital variation and the 6.5 day half-orbital variation, with additional sporadic outbursts or obscuration events, or both. The point X has the value $\Delta V = 5^m.74$ and is below the lower border of the figure; it indicates the lowest brightness ever recorded for SS 433 (*see text*). Underlying the rapid variations is the 162^d "precessional" variation; a fitted sine wave is shown to indicate this process. At the bottom of the figure we show relative magnitudes of the primary comparison star 1 against a secondary comparison star (check star) *a*, as measured somewhat intermittently over the six years at Pine Mountain; see text.

TABLE 1

V MAGNITUDES OF SS 433 RELATIVE TO STAR 1

JD	Δm		JD	Δm		JD	Δm		JD	Δm		JD	Δm		JD	Δm
4076.850	2.930		4418.800	2.837		4458.380	3.000	W	4521.982	3.107	K	4835.739	2.740		5173.872	2.849
4078.400	3.230	W	4419.900	3.379		4458.780	2.934		4526.941	2.463	K	4836.338	2.911	W	5174.787	2.903
4078.840	3.030		4421.800	3.235		4459.380	2.830	W	4527.948	2.450	K	4837.748	2.671		5175.793	3.123
4105.370	2.690	W	4423.800	3.126		4459.750	2.749		4531.699	2.780		4838.311	2.620	W	5176.799	3.136
4106.310	2.860	W	4427.800	3.184		4460.810	2.768		4535.609	2.239		4838.837	2.505		5179.879	2.851
4107.330	2.520	W	4428.800	2.644		4461.012	2.757	K	4540.937	2.857	K	4839.312	2.613	W	5181.761	3.168
4108.370	2.580	W	4429.480	2.600	W	4461.780	2.513		4541.935	2.903	K	4839.792	2.451		5182.869	2.815
4109.790	2.590		4429.900	2.740		4462.061	2.747	K	4542.921	2.740	K	4843.705	3.596		5183.786	3.111
4110.800	2.930		4430.470	2.630	W	4462.770	2.559		4543.927	2.610	K	4844.700	2.995		5184.850	2.673
4119.810	2.940		4431.430	2.890	W	4463.044	2.970	K	4544.930	2.473	K	4847.773	3.114		5187.762	2.760
4121.750	2.270		4431.800	2.847		4463.730	3.091		4547.934	2.663	K	4848.733	3.162		5193.792	2.255
4122.770	2.700		4432.520	3.000	W	4464.105	3.228	K	4698.577	2.896	W	4850.327	3.064	W	5194.744	2.143
4123.760	3.280		4433.480	2.840	W	4464.740	2.807		4725.290	2.860	W	4850.691	3.071		5195.795	2.663
4124.740	2.950		4433.900	2.783		4465.989	2.717	K	4729.233	2.846	W	4851.334	2.810	W	5197.861	2.465
4125.750	3.020		4434.470	2.730	W	4467.076	2.427	K	4730.530	2.917	W	4852.326	2.792	W	5198.826	2.494
4126.740	2.860		4435.410	2.670	W	4468.090	2.592	K	4743.218	2.890	W	4353.200	2.750	W	5199.745	2.386
4127.750	2.550		4435.700	2.478		4468.770	2.412		4753.230	3.270	W	4853.300	3.016	W	5200.821	2.681
4128.740	2.610		4436.210	2.510	K	4470.750	2.742		4770.901	2.866		4854.200	3.000	W	5201.867	2.603
4129.280	2.840	W	4436.350	2.580	W	4471.750	2.377		4784.492	2.722	W	4854.248	3.605	W	5202.786	2.816
4129.740	3.110		4436.700	2.405		4472.790	2.465		4785.455	2.698	W	4854.708	3.511		5203.803	2.462
4130.300	2.960	W	4437.066	2.585	K	4474.790	2.343		4786.398	2.614	W	4854.790	3.120		5204.814	2.750
4130.740	3.150		4437.280	2.710	W	4475.760	2.823		4787.337	4.497	W	4855.697	3.352		5205.770	3.018
4131.710	2.830		4437.700	2.902		4476.680	3.169		4788.398	2.389	W	4855.778	3.526		5206.775	2.892
4132.790	2.890		4438.198	3.113	K	4477.750	3.011		4789.413	2.613	W	4855.840	3.033		5207.745	3.106
4133.300	2.740	W	4439.127	2.745	K	4478.750	2.344		4790.389	3.185	W	4856.706	3.178		5208.761	3.085
4133.700	2.690		4439.800	2.829		4480.750	2.388		4791.400	3.144	W	4856.828	3.120		5209.854	3.763
4134.300	2.760	W	4440.149	2.925	K	4483.013	2.554	K	4792.397	2.632	W	4857.247	2.999	W	5212.859	3.209
4134.720	2.680		4440.800	2.928		4483.740	2.480		4793.477	2.401	W	4857.707	3.361		5213.813	2.497
4136.690	2.990		4441.137	2.929	K	4484.024	2.547	K	4794.365	2.363	W	4858.728	2.728		5216.727	2.878
4137.700	2.980		4441.800	2.986		4484.720	2.398		4799.875	2.548		4858.852	2.548		5217.721	2.854
4139.730	1.810		4442.134	2.840	K	4485.009	2.441	K	4800.818	2.294		4859.274	3.078	W	5218.705	2.660
4140.710	2.410		4442.800	3.127		4485.780	2.386		4801.783	2.405		4859.724	3.088		5219.701	2.850
4141.720	2.600		4443.132	2.720	K	4486.020	2.314	K	4803.815	3.238		4859.835	2.223		5220.788	2.859
4143.680	2.570		4443.800	3.107		4486.310	2.370	W	4805.410	2.490	W	4860.231	2.897	W	5221.806	3.357
4146.690	2.310		4444.800	3.019		4487.044	2.340	K	4805.729	2.465		4860.723	2.972		5222.815	3.649
4147.710	2.500		4445.800	2.752		4487.380	2.330	W	4806.402	2.504	W	4860.830	2.456		5223.713	2.916
4148.700	2.580		4446.800	2.974		4487.720	2.361		4806.771	2.368		4861.750	3.617		5226.731	2.084
4149.680	2.830		4447.800	2.490		4489.046	2.848	K	4807.722	2.473		4862.719	3.210		5233.682	2.488
4150.670	2.640		4448.800	2.867		4489.974	3.130	K	4808.770	2.565		4863.245	2.967	W	5234.767	2.642
4151.660	2.430		4449.800	2.739		4490.730	3.280		4809.774	2.617		4863.732	2.864		5235.684	5.740
4154.690	2.240		4450.800	2.751		4491.045	2.700	K	4810.764	2.974		4864.279	2.831	W	5237.787	2.948
4155.710	2.510		4451.800	3.022		4491.690	2.470		4811.764	2.461		4864.678	3.117		5238.689	2.964
4156.670	2.560		4452.800	3.194		4493.730	2.395		4812.769	2.418		4865.221	2.865	W	5243.678	3.279
4157.680	2.430		4453.800	3.101		4494.700	2.417		4813.802	2.031		4867.280	3.097	W	5244.670	3.145
4159.660	2.330		4454.810	2.290		4496.014	2.465	K	4814.774	2.512		4868.245	3.309	W	5252.717	2.982
4165.230	2.510	W	4455.310	2.750	W	4497.020	2.494	K	4815.833	2.535		4869.297	3.417	W	5253.699	2.783
4166.240	2.410	W	4455.790	2.941		4497.270	2.560	W	4816.762	3.073		4870.231	3.326	W	5254.677	3.056
4172.620	2.320		4456.101	2.746	K	4498.020	2.393	K	4817.854	2.645		4870.720	2.984		5255.698	3.216
4173.610	2.420		4456.770	2.685		4498.380	2.480	W	4818.771	2.683		4871.664	3.096		5259.715	2.825
4174.620	2.540		4457.360	2.980	W	4498.790	2.035		4819.391	2.498	W	4878.670	3.150		5260.649	2.809
4175.240	3.280	W	4457.900	2.890		4499.033	2.367	K	4819.932	2.776		4879.663	3.336		5261.635	3.376
4378.000	3.352		4178.650	1.840		4499.270	2.440	W	4820.388	2.458	W	4882.708	3.356		5266.637	2.418
4378.900	3.169		4184.620	2.300		4499.670	2.269		4820.781	2.500		4893.649	3.056		5273.680	2.751
4380.000	2.880		4185.620	2.830		4500.280	2.450	W	4821.391	2.570	W	4895.657	3.391		5274.665	3.212
4381.000	2.888		4187.650	3.110		4500.740	2.299		4821.773	2.582		4896.636	3.495		5275.637	3.183
4383.000	2.432		4188.630	3.020		4501.800	3.400		4822.391	2.561	W	4899.649	2.572		5276.640	2.616
4385.520	3.400	W	4189.630	2.550		4504.670	2.728		4822.826	2.346		4900.661	2.701		5278.608	2.450
4387.550	3.800	W	4190.640	2.350		4505.643	2.485		4823.382	2.755	W	4902.653	3.031		5280.620	2.572
4388.000	2.976		4191.640	2.250		4506.647	2.558		4823.805	2.786		4909.657	3.625		5284.612	2.466
4389.000	3.003		4192.600	2.190		4509.687	3.124		4824.396	2.820	W	4910.647	3.581		5287.622	3.109
4389.900	2.854		4197.620	2.220		4511.988	2.500	K	4824.812	2.436		4911.618	2.739		5288.655	3.125
4390.900	3.121		4198.610	2.260		4512.978	2.524	K	4825.819	2.356		4913.616	2.845		5297.614	2.332
4392.900	3.121		4202.620	3.280		4513.676	2.501		4826.756	2.236		4915.622	3.065		5440.976	2.543
4397.900	3.600		4213.600	1.950		4513.977	2.756	K	4827.770	2.600		4916.629	3.291		5441.948	2.390
4398.900	3.119		4216.590	2.680		4514.718	1.858		4828.348	2.717	W	4937.621	2.542		5457.948	2.894
4400.900	4.174		4348.000	3.071		4515.704	2.793		4828.760	2.852		5153.887	3.170		5458.919	2.488
4401.900	2.140		4355.000	2.000		4515.978	3.320	K	4829.371	3.253	W	5154.881	2.438		5466.924	2.876
4405.900	2.850		4357.000	2.381		4516.699	3.559		4830.281	3.610	W	5155.859	2.645		5468.899	2.749
4406.900	2.938		4358.000	2.906		4516.981	3.225	K	4830.898	3.321		5161.942	3.659		5473.901	2.310
4407.520	3.310	W	4360.900	3.600		4517.290	3.060	W	4831.345	2.884	W	5162.817	3.542		5474.898	2.351
4408.440	3.440	W	4364.000	2.675		4517.693	2.645		4831.710	2.663		5163.861	3.296		5475.931	2.885
4408.800	3.329		4365.000	2.827		4518.260	2.900	W	4832.377	2.749	W	5165.858	2.224		5476.875	2.235
4409.400	3.090	W	4372.000	3.131		4518.774	2.447		4832.726	2.537		5167.783	2.712		5480.839	2.442
4409.800	3.256		4375.000	3.104		4519.650	2.893		4833.347	2.620	W	5168.848	2.910		5481.921	2.716
4410.390	3.370	W	4376.000	2.985		4520.702	2.657		4833.729	2.609		5169.865	3.240		5482.911	3.006
4411.900	3.829		4377.000	2.772		4520.965	2.904	K	4834.849	2.694		5170.873	3.275		5484.896	3.327
4417.800	3.044					4521.731	3.015					5172.816	2.856			

TABLE 1—*Continued*

JD	Δm		JD	Δm		JD	Δm		JD	Δm		JD	Δm	
5487.854	2.326		5836.879	3.135		5940.063	2.553	K	6036.607	2.540		6265.756	2.359	
5488.828	2.649		5838.910	3.455		5940.707	2.756		6039.592	2.345		6266.781	2.527	
5489.940	2.298		5847.898	2.677		5940.827	2.732	M	6040.590	2.630		6269.762	3.170	
5490.891	2.670		5848.861	3.190		5940.839	2.807		6133.610	2.822	W	6270.749	2.442	
5491.903	2.598		5849.888	3.491		5941.025	2.853	T	6134.600	2.247	W	6271.036	2.424	K
5492.809	2.428		5854.841	2.728		5941.062	2.894	K	6152.590	3.201	W	6271.755	2.407	
5496.816	3.232		5859.857	3.437		5941.750	3.096		6154.540	3.175	W	6272.753	2.240	
5497.931	2.324		5868.846	2.919		5941.821	3.061		6157.005	3.156		6273.810	2.370	
5498.818	2.325		5878.850	3.512		5941.829	3.126	M	6157.983	3.202		6276.380	2.527	W
5499.867	2.589		5879.844	3.236		5942.053	3.203	K	6159.007	3.005		6277.290	2.417	W
5500.879	2.031		5881.856	2.845		5942.756	3.072		6160.959	2.987		6278.280	2.380	W
5501.855	2.362		5882.875	2.992		5942.840	2.919	M	6161.985	3.073		6278.896	2.289	
5509.880	2.682		5883.843	3.510		5943.016	2.963	K	6163.990	3.527		6279.370	2.643	W
5513.880	2.359		5884.851	3.311		5943.835	2.532	M	6164.976	3.477		6279.767	2.310	
5518.974	2.628		5885.922	3.259		5944.033	2.529	K	6165.949	3.310		6280.290	2.435	W
5519.771	3.015		5886.871	2.926		5944.098	2.528	T	6166.996	3.189		6280.774	2.513	
5520.825	3.037		5887.844	3.384		5944.822	2.445	M	6168.954	3.164		6281.270	3.070	W
5521.848	2.599		5888.837	3.377		5944.827	2.581		6169.947	2.634		6281.817	3.022	
5522.802	3.532		5889.816	3.788		5945.713	2.571		6171.550	3.137	W	6282.250	3.283	W
5525.813	3.123		5890.769	3.550		5945.832	2.451		6172.510	2.787	W	6283.320	2.977	W
5526.785	2.826		5890.935	3.237		5946.050	2.394	T	6174.490	3.370	W	6283.764	2.604	
5527.817	3.126		5891.803	3.308		5946.108	2.419	K	6175.976	3.401		6284.350	2.462	W
5531.814	3.031		5892.847	3.291		5946.717	2.386		6177.940	3.504		6284.742	2.391	
5533.747	2.983		5893.783	2.949		5947.155	2.408	K	6181.949	3.158		6285.500	2.569	W
5536.793	3.280		5894.794	2.825		5947.725	2.460		6182.936	2.880		6285.842	2.391	
5537.768	3.031		5895.798	2.713		5951.717	2.393		6185.969	3.318		6286.240	2.576	W
5538.847	2.884		5896.783	2.699		5952.768	2.468		6189.929	3.480		6286.749	2.495	
5539.784	3.621		5898.871	2.659		5953.824	2.622		6190.935	3.008		6287.720	2.537	
5541.769	2.968		5899.884	3.101		5955.762	3.043		6197.952	3.315		6288.780	2.670	
5543.849	3.340		5900.847	3.268		5956.746	2.492		6198.906	3.478		6289.767	2.389	
5544.749	3.448		5901.794	3.283		5957.705	2.400		6203.866	3.493		6290.771	2.460	
5545.755	3.105		5902.816	3.341		5958.792	2.344	M	6204.936	3.294		6291.752	2.504	
5548.761	3.494		5906.750	2.945		5959.719	2.343		6206.900	2.957		6291.846	2.401	
5549.799	3.581		5907.787	2.649		5960.711	2.558		6207.906	2.846		6292.793	2.567	
5550.792	3.170		5908.840	3.128		5961.697	2.584		6208.920	2.940		6293.756	2.767	
5551.828	2.809		5909.775	3.288		5963.782	2.403		6209.930	2.850		6294.751	3.257	
5552.797	3.059		5911.818	2.245		5964.712	2.447		6211.868	3.380		6296.036	3.184	K
5553.817	1.675		5912.812	2.574		5965.220	2.470	W	6212.842	3.363		6296.747	3.017	
5555.907	2.334		5915.845	2.810		5965.731	2.374		6215.912	3.481		6297.142	3.059	K
5557.861	3.033		5917.851	2.629		5966.016	2.365	K	6219.822	3.033		6299.787	2.876	
5558.778	1.902		5918.822	2.327		5966.987	2.641	K	6225.882	3.055		6300.743	2.886	
5559.809	2.870		5919.866	2.495		5968.040	3.093	K	6226.876	3.133		6302.727	2.952	
5561.758	3.347		5920.770	2.419		5968.725	2.956	M	6227.840	3.183		6303.756	2.791	
5563.759	3.482		5921.844	2.486		5969.748	3.145		6228.859	3.519		6314.716	3.180	
5567.770	2.631		5924.843	2.661		5969.023	2.926	K	6229.830	3.705		6320.050	3.259	K
5568.834	3.219		5925.809	2.566		5969.677	2.753		6230.868	3.341		6321.045	3.509	K
5570.788	3.280		5927.784	2.722		5969.757	2.720		6231.883	3.279		6327.270	3.227	W
5571.745	3.312		5929.806	2.891		5969.974	2.658	K	6232.870	2.984		6327.673	3.435	
5573.729	2.932		5930.117	2.633	T	5970.005	2.639	T	6233.869	2.641		6328.796	3.097	
5579.782	2.944		5930.733	2.615		5970.694	2.677		6234.843	2.653		6330.771	2.995	
5580.717	2.386		5930.873	2.549		5970.777	2.626		6236.925	2.935		6331.777	3.268	
5582.736	2.680		5931.063	2.498	T	5970.987	2.640	T	6237.380	3.053	W	6333.668	3.452	
5583.712	2.744		5931.767	2.437		5970.991	2.651	K	6237.922	2.874		6334.663	3.210	
5584.722	2.853		5931.966	2.358		5971.687	2.689		6238.905	3.147		6336.720	3.328	
5585.742	2.993		5932.079	2.320	T	5971.997	2.602	T	6239.320	3.230	W	6339.688	3.823	
5586.759	2.633		5932.738	2.316		5972.097	2.657	K	6244.900	2.794		6341.684	3.044	
5587.740	3.524		5932.838	2.423		5972.774	2.769		6246.936	2.625		6342.667	3.084	
5590.691	2.843		5933.714	2.345		5972.792	2.676	M	6249.938	3.120		6343.300	3.401	W
5591.760	1.943		5933.794	2.481		5973.750	2.818		6251.440	3.104	W	6344.330	3.203	W
5592.792	2.074		5933.847	2.649		5973.979	2.725	T	6251.897	2.657		6344.667	3.283	
5595.792	2.456		5934.745	2.542		5974.700	3.034		6252.260	2.759	W	6348.717	3.259	
5597.699	2.597		5934.839	2.491		5974.967	3.041	K	6253.280	2.766	W	6351.711	3.060	
5598.686	2.705		5935.088	2.554	K	5975.644	3.018		6253.926	2.486		6353.687	3.019	
5602.748	2.746		5935.711	2.689		5975.748	2.806		6255.956	3.324		6355.657	3.153	
5611.730	2.407		5935.805	2.833		5975.973	2.768	K	6256.950	2.907		6356.677	3.498	
5612.738	1.910		5936.076	2.673	K	5976.640	2.728		6258.280	2.769	W	6366.631	2.950	
5613.741	2.904		5936.721	2.660		5976.735	2.701		6259.947	2.575		6376.200	3.567	W
5619.660	2.402		5937.106	2.515	T	5976.962	2.657	K	6260.280	2.603	W	6383.622	3.334	
5623.743	3.144		5938.707	2.402		5977.730	2.568		6260.799	2.423		6392.605	3.550	
5631.673	2.465		5938.770	2.400		5981.667	3.435		6261.933	2.554		6394.626	3.527	
5633.652	2.430		5938.846	2.450		5985.643	2.881		6262.560	2.835	W			
5643.671	2.650		5938.883	2.604		5991.699	3.017		6262.838	2.574				
5806.002	2.573		5938.902	2.463	M	5995.684	3.372		6262.881	2.720				
5818.942	2.664		5939.702	2.460		6000.684	3.314		6263.300	2.711	W			
5825.927	2.878		5939.829	2.526		6003.605	2.938		6263.882	2.561				
5826.951	2.954		5939.863	2.458	M	6026.648	2.720		6264.815	2.470				
5827.943	2.879					6030.601	2.756							

NOTES.—Data Sources: unlabeled = Pine Mountain Observatory; W = Wise Observatory; K = Kagoshima Space Center; T = Tokyo Astronomical Observatory; M = Mauna Kea Observatory.

and Okazaki). Results from that effort, which were exciting and extremely important, will be published elsewhere (Stewart *et al.* 1986) and will be mentioned in our discussion below.

Observing time scales—The data values in Table 1 are generally averages from data collected over the span of 30–90 minutes. In most cases, especially at PMO and Wise Observatory, only one sample, a mean measure over ~ 1 hour, was taken per night. Exceptions will be seen in Table 1, e.g., during the 1984 special campaign. In cases where the object was observed with one telescope for several hours in a night, we have condensed the data integrations into ~ 1 hour averages. This condensation tends to make the data set, as given in Table 1, more homogeneous and uniform. In fact, the shortest time scale for appreciable variability in SS 433 seems to be 1–2 hours, with rare exceptions. (A separate analysis of variation on time scales from 30 minutes to days, as revealed by the 1984 campaign is being carried out by the Japanese group.)

Measuring errors—We do not list the individual errors in Table 1, partly because we could not do this in a uniform way. The methods of computing errors were different among the three observing groups. The PMO photometer is an analog type with A/D conversion to digital signals; errors are computed from fluctuations among actual magnitudes measured over a series of five-minute complete sequences of type object–sky comparison. Such errors include all sources of error such as variable sky, as well as photon statistics. The Japanese and Israeli observations were done with pulse-counting photometers, and usually only the photon-statistical errors were tabulated. The real errors for the great majority of points in Table 1 lie in the range $0^m.03$–$0^m.15$, with a most typical error of perhaps $0^m.07$–$0^m.08$. When the object was very faint the errors tended to be large, when expressed in magnitudes. For analyzing the periodic effects (13^d and 162^d cycles, etc.), and for power-spectrum analysis, the individual errors are of course not needed. In the binned light curves what matters is only the spread among the data points within the phase bins.

b) *A Simple or Real-Time Plot of the Light Variation, 1979–1985*

This is shown in Figure 1, in terms of the magnitude difference $\Delta V = V(\text{SS } 433) - V(1)$, where $V(1)$ is the magnitude of our main comparison star. We use an inverted vertical scale so that the brightness of SS 433 is upward. In this figure, the data points are connected arbitrarily with straight-line segments.

The relatively rapid, spikelike fluctuations on a time scale of 6-13 days are largely due to the 13 day eclipsing-binary cycle. But there are also erratic spikes and dips seemingly due to flaring or obscuration events or both. The extreme example is the point X, which is actually below the bottom of the plot.

Underlying the rapid variation is the 162 day "precession" cycle. In Figure 1 we indicate that with a fitted sine wave, using the best-fit period of $162^d.5$ (see below). On the whole this fit is visually convincing.

The point X, which is actually below the lower border of the figure, indicates *the lowest brightness ever recorded* for SS 433. It occurs at JD 2,445,235.684, at precisely orbital phase $\phi = 0.0$, primary minimum (see Fig. 3), and at precession phase $\Phi = 0.11$. The actual value is $\Delta V = 5^m.74 \pm 0.70$. The error in magnitude is misleading because the object's brightness in *intensity* units is only 0.07 times the mean or typical brightness corresponding to about the level $\Delta V = 2^m.8$. Relative to unit intensity at the mean level, the point X has intensity 0.069 ± 0.131, which is over 7 standard errors below the mean level. This measurement at PMO was a 30 minute integration on a clear night with no special problems.

III. THE PERIODIC PROCESSES IN THE LIGHT VARIATION

a) *Power Spectrum, Periods, and New Ephemerides*

In Figure 2 we show a power spectrum of the SS 433 V-band light variation. This was computed by the Fourier summation method, which is done by computing:

$$C_\gamma = \frac{2}{N}\sum_i^N (\Delta V)_i \cos(2\pi\nu t_i) ,$$

$$S_\gamma = \frac{2}{N}\sum_i^N (\Delta V)_i \sin(2\pi\nu t_i) ,$$

and by then computing $A_\gamma^2 = C_\gamma^2 + S_\gamma^2$, the spectral power. Here i sums over the N data points, for a sequence of frequencies $\nu = 1/P$. In Figure 2 we use 2000 search frequencies out to $P_{\min} = 6.0$ days.

In Figure 2 the highest peaks have periods of ~ 162 and 6.54 days. The second of these is the half-orbital period, i.e., half of 13.08 days. A strong peak is also seen at the full orbital period. Nearby alias peaks or sidebands, caused by gaps in the data during winters, are also present. A higher resolution version of this power spectrum gives an updated best-choice precession period of $162^d.5 \pm 0^d.25$, as an average for the six years.

Phasing of the 162^d light and radial-velocity variations.—While the 162^d light curve is not simply sinusoidal, the principal Fourier component is a 162 day sine wave. We denote the epoch T_0 and precession phase $\Phi = 0.0$ as the time of light minimum in terms of the 162^d Fourier component, as in Henson *et al.* (1983) and previous papers. In the present data set, we found an epoch $T_0 = \text{JD } 2{,}440{,}017.9$, using at least-mean-squares fit to a $162^d.5$ sinusoid. Anderson *et al.* (1983*b*), using the period $162^d.7$, give the epoch $t_0 = \text{JD } 2{,}443{,}561.8$ as the time of "first crossover" of the moving Balmer emission lines. This time is ~ 26 days before the centroid or mean time between the two crossovers.[1] Adding 26 days to the Anderson *et al.* t_0 we compute a central epoch (with $\Phi = 0.0$) of JD 2,445,214.8 for the radial-velocity cycle, near the mid point of the 1979–1985 interval, using precisely the $162^d.7$ period. The corresponding central epoch for the light variation, using a $162^d.5$ period, is $T_0 = \text{JD } 2{,}445{,}217.9$. The agreement here to within 3 days is probably better than we could expect.

New emphemeris for the orbital light variation, and a mean light curve.— We found the best-fit 13^d period by first subtracting off an average $162^d.5$ sinusoid from the ΔV values, which removes most of the variance due to that cycle. Least-mean-square fits were then made to a sum of full-period and half-period sinusoids (five-term regression including a constant), over a range of periods $\sim 13^d.08$. The highest Fisher F statistic for this fit was found with $P = 13^d.081 \pm 0^d.003$.

In Figure 3 we show the mean 13^d light curve, with 20 bins, on the $13^d.081$ period, using the entire data set of Table 1 except for a handful of late 1985 points[2]. A $162^d.5$ sine wave has

[1] We feel it was a little unfortunate that a symmetrical phase convention was not adopted in the radial-velocity studies of the 162^d variation. The symmetrical choice is to designate the epoch ($\Phi = 0$) as the central time between adjacent crossovers of the moving lines, which is effectively what we do here; with this phasing, light maximum and also maximum separation of the pairs of moving lines occur at $\Phi = 0.5$.

[2] About 30 late data points were not used; these were added to our files after Figs. 2–4 were made up.

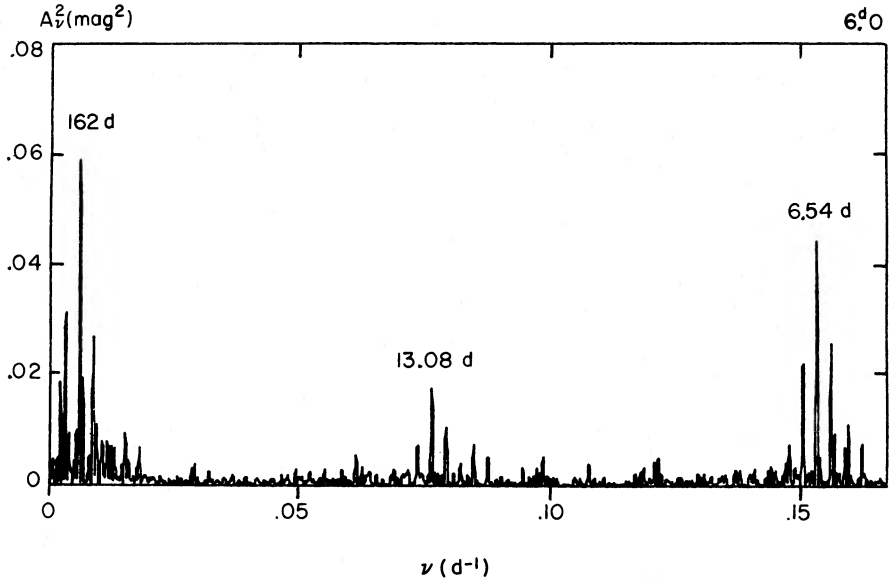

FIG. 2.—Power spectrum of the V-band light variation in SS 433, based on 783 data points during 1979–1985. The abscissa is in frequency (inverse period), out to a shortest period of 6.0 days. Sidebands or extra peaks around the principal high peaks are largely spurious, caused by approximately five month gaps between observing seasons.

been subtracted to reduce the bin errors. The bin errors here, also in the binned curves of Figure 4, were computed from the expression $\sigma/(N-1)^{1/2}$, where σ is the standard deviation of the data points in a bin around the bin average and N is the number of points in the bin.

From the mean curve we find primary light minimum to occur at epoch JD 2,440,003.434, and we have defined the phase $\phi = 0.0$ in Figure 3 to correspond with that. Note the curve's approximate mirror symmetry around $\phi = 0.5$ (and $\phi = 0$); secondary light minimum occurs quite accurately at $\phi = 0.5$.

b) "Precessional" Light Curves: Breakdown by Orbital Phases

Several 160 day light curves using earlier data sets have appeared in print. The 160 day variation was early recognized to be sensitive to the 13 day cycle (and vice versa), and a simple curve averaged over orbital phase omits key information on the structure of the system. We would like to "freeze" the precessing disk, in a manner of speaking, at given orbital phases and watch it precess in space without orbital motion. This can be done in effect by sorting the data into orbital phase bins, as was done in a coarse way by Leibowitz *et al.* (1984*b*) and more recently by Antokhina and Cherepashchuk (1985). But in the former of those cases, only a breakdown into two halves of the orbital cycle was done, while in the second case, bin errors were not shown and one could not assess the statistical significance of the curves.

With the present six-year data train it is fruitful to carry out this decomposition in more detail. In Figure 4 we show $162^d.5$ light curves segregated into four orbital phase bins of full widths 0.2 cycle, centered on: $\phi = 0$ (primary minimum), 0.25, 0.5 (secondary minimum), and 0.75.

Note the upward "hump" in the 162^d light curve around precession phase $\Phi = 0$, in the curve with mean orbital phase 0.5—*secondary* 13^d light minimum. Only traces of such a hump, without statistical significance, are seen in the curves for other orbital phases. This finding is extremely significant for geometrical models of SS 433 and will be taken up in dis-

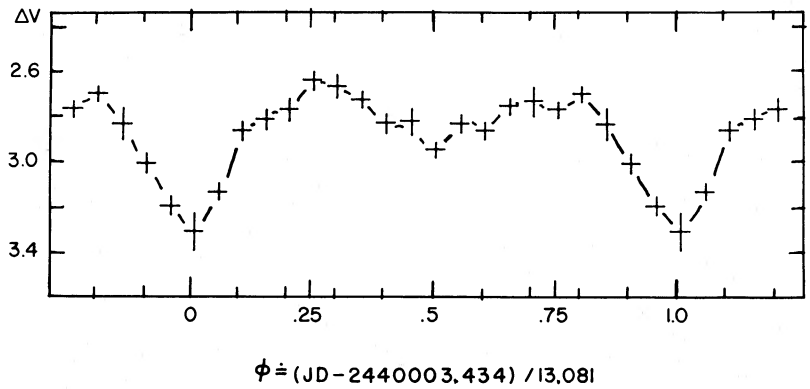

FIG. 3.—The mean V-band light curve on the orbital period $13^d.081$, using 783 data points from 1979–1985. To reduce the variance within phase bins, the underlying 162 day variation has been subtracted by removing a $162^d.5$ regression-determined sinusoid. In this and also Fig. 4, the bin errors are computed from the variances of data points within the bins; a bin error is computed at $\sigma/(N-1)^{1/2}$, where σ is the standard error (root-mean-square fluctuation) of the N points in the bin.

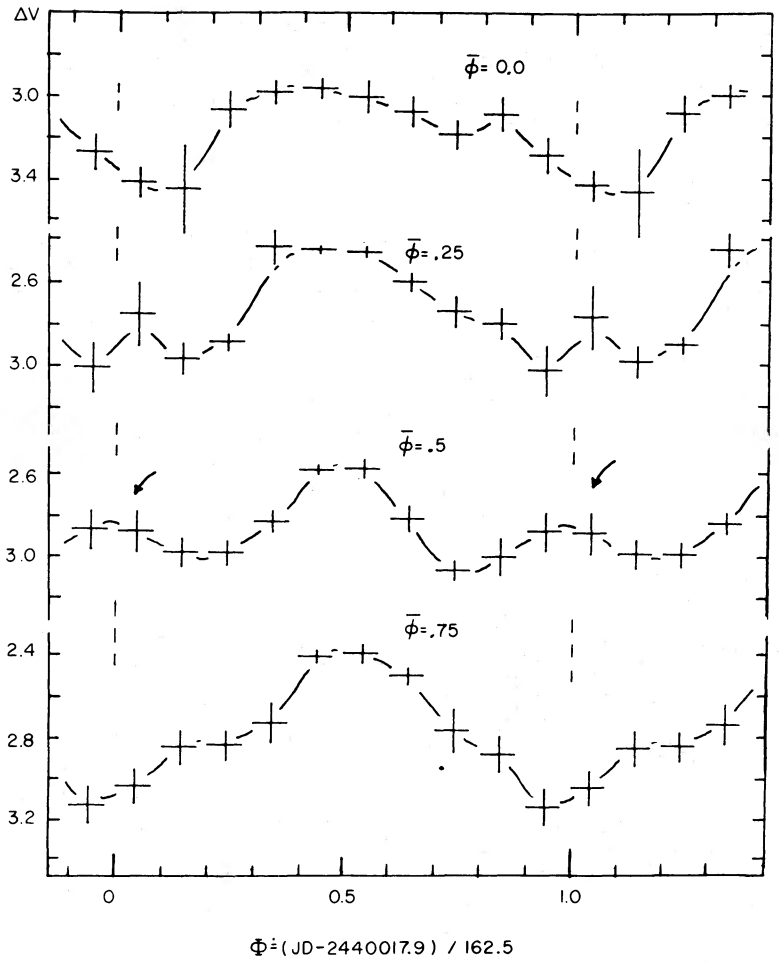

FIG. 4.—Decomposition of 162^d.5 light curves into phase intervals of widths $\Delta\phi = 0.2$ of the 13^d orbital period, centered on four orbital phases ϕ: 0.0 (primary minimum) 0.25 (first quadrature) 0.5 (secondary minimum) 0.75 (second quadrature). The arrow points to a brightness "hump" in the precessional light curve at precession phase $\Phi = 0$, which occurs most clearly at or near orbital phase 0.5, when the secondary body (collapsed body and disk) are presumed to be in front of the star.

cussion below. Hints of this sort of structure were seen in earlier work Mazeh, Leibowitz, and Lahav 1981; Henson *et al.* 1983) but here the feature is quite definite.

IV. DISCUSSION

A primary reason for this paper is to provide the community with a long, homogeneous data base of the complex light variation in this object. However, we have included a modest amount of synthesis of the data, and some remarks follow.

The "hump" in the precession light curve noted above is an especially interesting feature which is fairly clear in our synthesis (Fig. 4).

In the model of SS 433 believed by many (but not all) investigators, we have a compact body, likely to be a black hole (Leibowitz *et al.* 1984*a*; Antokhina and Cherepashchuk 1985), orbiting an evolved star which fills its Roche lobe. A precessing disk and associated beams which issue normally from the disk's nucleus are centered on the compact body. Variants of mechanisms underlying the precession have been described by Leibowitz (1984). The system's orbital inclination is 78°–80°, and it is clearly an eclipsing system. The disk tilt angle out of the orbital plane is $\sim 20°$.

A question which was asked as soon as the eclipsing binary-like 13^d light curve was defined was: "What is eclipsing what, at primary minimum in this light curve?" Unlike the situation with less exotic binary objects, this question could not be quickly answered, mainly because spectral lines from the presumed mass-losing star in the system have not been definitely identified. The best case for lines showing orbital motion seems to be that of the He II line at 4686 Å, which Crampton and Hutchings (1981) propose to originate in the accretion disk. Those lines show velocity variations which are in an approximately quadrature relationship to the light-curve minima. The maximum positive He II radial velocity occurs at close to our orbital phase 0.75. If the λ4686 line originates in the disk, this says that the disk is "behind" the star at primary light minimum, $\phi = 0$. Confirmation of that phasing seems to come from Katz *et al.* (1982), from an analysis of the so-called nodding motion of the precessing disk.

That the disk is behind the (darker) star at $\phi = 0.0$ has recently become quite certain from dramatic results of joint X-ray/optical observations, in 1984, which we mentioned in § II*a* above (a paper, Stewart *et al.* 1986, is in preparation). The 13 day X-ray light curve was found, in fact, to show a definite minimum at orbital phase 0; the source is (partially) obscured around that phase.

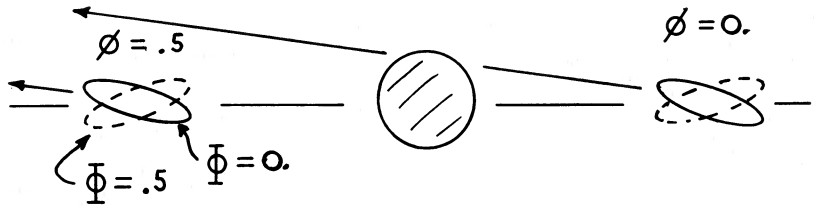

FIG. 5.—Some geometrical aspects of the system, relevant to the appearance of the brightness hump in the precessional light curve at precession phase 0.0 referred to in Fig. 4 and in the text. This is a view of the system from a vantage point in the orbital plane, moved out at right angles to the object-Earth direction. The disk is represented as having a thick elliptical cross section. The observer (at Earth) is off to the left in the figure. Solid-line ellipses represent the disk cross section at precession phase $\Phi = 0$, when we tend to look "under" the disk. Dashed-line ellipses represent precession phase 0.5, when the disk presents a maximum cross section to us—and when, also, the "moving" Balmer emission-line pairs due to the beams (not shown in the figure) are most widely separated.

Assuming this phasing of the system's components, let us look at the hump in the 162 day light curve at $\Phi = 0$, which is visible when the orbital phase is around 0.5. We attempt to interpret this in terms of the geometry of Figure 5. There we depict the SS 433 system as seen from the side, from a vantage point in the system's orbit plane but moved out at right angles to the object-Earth direction. At $\phi = 0.5$, the disk is not eclipsed at *any* precession phase (Φ) by the star. Let us assume that the disk luminosity and the luminosity distribution over the disk do not depend on either ϕ or Φ. The disk is taken to be optically thick. When both ϕ and Φ equal ~ 0.5, we have an absolute light maximum, with the disk presenting a maximum, unobscured cross section to us. At about precession phases $\Phi = 0.25$ and 0.75, the disk is edge-on, causing light minima. At orbital phase $\phi = 0.5$, and at $\Phi = 0.0$ we actually look "under" the disk and see the luminous underside producing a second, small light maximum—a hump in the precessional light curve.

The situation is different at orbital phase 0. Since we do not see the brightness hump at $\Phi = 0$ in that case, we must suppose that the bright underside of the disk is covered by the star—at least the central part of the underside, which is the hottest and brightest part.

This qualitative picture of the hump phenomenon seems to require, for one thing, that the disk is geometrically thick. Antokhina and Cherepashchuk (1985) have modeled the light curves using essentially the above physical picture. They used a (thick) precessing ellipsoid for the accretion disk, with a high polar temperature which they place in the range 20,000–100,000 K. They took the primary star to be an OB star with $T \approx 16{,}000$ K. From their modeling they find a pattern which partly agrees with our observed curves: They show precession curves with a "hump" at $\Phi = 0$ (or $\alpha = 180°$ in their notation) for the case $\phi = 0.5$ (orbital secondary minimum) but almost no hump for $\phi = 0$.

The agreement of our curves with the above picture is not complete. A hump at $\Phi = 0$ ought to be seen at *all* orbital phases *except* near $\phi = 0$, where the disk is partly eclipsed. The model curves of Antokhina and Cherepashchuk for quadrature orbital phases show an undiminished hump. But the quadrature-phase curves in our Figure 4 show only a mild hump (which may not even be statistically significant) for $\phi = 0.25$, and none at all for $\phi = 0.75$. Something else must be involved. Back heating of the primary star by the disk could have a subtle effect: at the orbital quadratures, when the disk is tipped at precession phase 0.0 it is edge-on to the star. The back heating and reflection by the star would be then reduced, and the resulting drop in the total light might cancel the brightness hump at $\Phi = 0$.

There is some evidence for certain asymmetries in the precession curves of Figure 4, e.g., in the $\phi = 0.25$ curve. Earlier precession light curves, based on fewer 162^d cycles, showed stronger asymmetries, but those features could have been an artifice of random or irregular intrinsic changes in the object. Asymmetrical precession and orbital light curves appear in model calculations by Leibowitz (1984), connected with a Coriolis-deflected gas stream and hot spot. It is worth noting, however, that our new mean 13^d light curve (Fig. 3), which has quite small bin errors, shows very little evidence for important asymmetry.

"*Dark*" *events and the disk luminosity.*—The extreme brightness drop at point X in Figure 1 and some other less-deep drops superficially suggest that the disk is very much brighter than the star. As noted in § II*b*, point X occurred at precisely $\phi = 0$, orbital primary minimum. Suppose the disk to vary somewhat in size from time to time and that it is normally eclipsed by, say, 80% at primary minimum. Then if the disk were momentarily 20% smaller at the time of some eclipse, it might literally disappear from view. If the drop at date X were taken literally it would imply that the disk is 13 times brighter than the star in visible light and certainly 4 times brighter allowing for statistical error. Another possibility for the dark events, however, might be external obscuration by a changing, surrounding dust cloud; Ramaty, Kozlovsky, and Lingenfelter (1984) discuss indirect evidence for the presence of dust grains near the SS 433 system, in connection with the gamma-ray emission mechanism. But it is worth noting (see data in Table 1) that one day before the point-X event, and two days after it, the object's brightness was normal; thus the time scale for an obscuring event would have to be short.

Further modeling of the SS 433 system is encouraged. We note that we have not searched the present data base for photometric counterparts of processes such as the nodding motion of the beams and disk (Katz *et al.* 1982), nor for indications of period changes. Readers are invited to analyze our data for such effects.

The Pine Mountain program on SS 433 is supported by National Geographic Society grant 3003-84 and by NSF grant AST-8405542. The work on SS 433 at Wise Observatory is partially supported by the Israeli Academy of Sciences. The Japanese group would like to thank M. Eiraku, M. Koyano, A. Okazaki, T. Omodaka, A. Yamasaki, and M. Yutani for their help with some of the observations and data reductions. One of us (J. C. K.) thanks N. Bochkarev and E. Karitskaya for important discussions and Bruce Margon and David Crampton for some comments.

REFERENCES

Anderson S. F., Margon, B., and Grandi, S. A. 1983*a*, *Ap. J.*, **269**, 605.
———. 1983*b*, *Ap. J.*, **273**, 697.
Antokhina, E. A., and Cherepashchuk, A. M. 1985, *Pis'ma Astr. Zhur.*, **11**, 10.
Cherepashchuk, A. M. 1981, *M.N.R.A.S.*, **194**, 761.
Crampton, D., Cowley, A. P., and Hutchings, J. B. 1980, *Ap. J.* (*Letters*), **235**, L131.
Crampton, D., and Hutchings, J. B. 1981, *Ap. J.*, **251**, 604.
Gladyshev, S. A., Goranskii, V. P., and Cherepashchuk, A. M. 1985, *Astr. Zhur.*, in press (Vol. **62**).
Gladyshev, S. A., Korochkin, N. E., Novikov, I. D., and Cherepashchuk, A. M. 1979, *Astr. Tsirk.*, No. 1086, I-8.
Henson, G. D., Kemp, J. C., Barbour, M. S., Kraus, D. J., Leibowitz, E. M., and Mazeh, T. 1983, *Ap. J.*, **275**, 247.
Katz, J. I., Anderson, S. F., Margon, B., and Grandi, S. A. 1982, *Ap. J.*, **260**, 780.
Kemp, J. C., Barbour, M. S., Arbabi, M., Leibowitz, E. M., and Mazeh, T. 1980, *Ap. J.* (*Letters*), **238**, L133.
Kemp, J. C., Barbour, M. S., Kemp, G. N., and Hagood, D. M. 1981, *Vistas Astr.*, **25**, 31.
Leibowitz, E. M. 1984, *M.N.R.A.S.*, **210**, 279.
Leibowtiz, E. M., Mazeh, T., and Mendelson, H. 1984*a*, *Nature*, **307**, 341.
Leibowitz, E. M., Mazeh, T., Mendelson, H., Kemp, J. C., Barbour, M. S., Takagishi, K., Jugaku, J., and Matsuoka, M. 1984*b*, *M.N.R.A.S.*, **206**, 751.
Leibowitz, E. M., and Mendelson, H. 1982, *Pub. A.S.P.*., **94**, 977.
Margon, B. 1984, *Ann. Rev. Astr. Ap.*, **22**, 507.
Mazeh, T., Leibowitz, E. M., and Lahav, O. 1981, *Ap. Letters*, **22**, 185.
Ramaty, R., Kozlovsky, B., and Lingenfelter, R. E. 1984, *Ap. J.* (*Letters*), **283**, L13.
Stewart, G. C., *et al.* 1986, in preparation.

IAN C. BEARDSLEY, LYNN C. CARROLL, GARY D. HENSON, JAMES C. KEMP., and DANIEL J. KRAUS: Department of Physics, University of Oregon, Eugene OR 97403

J. JUGAKU: Tokyo Astronomical Observatory, Mitaka, Tokyo 181, Japan

ELIA M. LEIBOWTIZ, TSEVI MAZEH, and HAIM MENDELSON: Wise Observatory, Tel Aviv University, Ramat Aviv, Tel Aviv, Israel

M. MATSUOKA: Institute of Space and Astronautical Science, Komaba, Meguro-ku, Tokyo 153, Japan

T. TAKAGISHI: Faculty of Engineering, Miyazaki University, Miyazaki 880, Japan